Science of the Total Environment 979 (2025) 179486

Contents lists available at ScienceDirect

Science of the Total Environment

journal homepage: www.elsevier.com/locate/scitotenv

Cascading droughts: Exploring global propagation of meteorological to hydrological droughts (1971–2001)

Amit Kumar[a,b,*], Simon N. Gosling[a], Matthew F. Johnson[a], Matthew D. Jones[a], Albert Nkwasa[c,d], Aristeidis Koutroulis[e], Hannes Müller Schmied[f,g], Hong-Yi Li[h], Hyungjun Kim[i], Naota Hanasaki[j], Rohini Kumar[k], Wim Thiery[d], Yadu Pokhrel[l]

[a] School of Geography, University of Nottingham, UK
[b] UK Centre for Ecology and Hydrology, UK
[c] Water Security Research Group, Biodiversity and Natural Resources Program, International Institute for Applied Systems Analysis (IIASA), Laxenburg, Austria
[d] Department of Water and Climate, Vrije Universiteit Brussel, Brussels, Belgium
[e] School of Environmental Engineering, Technical University of Crete, Chania, Greece
[f] Institute for Physical Geography, University of Frankfurt, Frankfurt am Main, Germany
[g] Senckenberg Leibniz Biodiversity and Climate Research Centre (SBiK-F), Frankfurt am Main, Germany
[h] Department of Civil and Environmental Engineering, University of Houston, USA
[i] Moon Soul Graduate School of Future Strategy, Korea Advanced Institute of Science and Technology (KAIST), Daejeon, Republic of Korea
[j] Center for Climate Change Adaptation, National Institute for Environmental Studies, Tsukuba, Japan
[k] Department of Computational Hydrosystems, Helmholtz Centre for Environmental Research–UFZ, Leipzig, Germany
[l] Department of Civil and Environmental Engineering, Michigan State University, East Lansing, MI, USA

* Corresponding author at: School of Geography, University of Nottingham, UK.
E-mail address: amit1792kumar@gmail.com (A. Kumar).

https://doi.org/10.1016/j.scitotenv.2025.179486

Available online 23 April 2025

HIGHLIGHTS

- The study identified 1740 meteorological droughts (MD) and 1493 hydrological droughts (HD) globally for the period 1971–2001.
- Only 272 MD events propagating into 395 HD events, highlighting the rarity of MD-to-HD propagation.
- A new technique using spatio-temporal overlap of MD and HD events was developed to quantify drought propagation and analyse propagation features.
- Long-term MD events (having duration of more than 12-months) were more likely to propagate, while propagated MD events exhibited reduced size, attenuated intensity, positive lag, and negative lengthening.
- Propagated MD events often displayed pooling, with a strong tendency for pooling events to also show branching behaviour.
- Among the 20 most severe MD events (largely aligned with literature), most propagated, showed positive lag, and diverged from general tendency by exhibiting positive lengthening.
- Africa and South America showed higher occurrences of pooling and branching due to favourable climatic and catchment conditions, while Asia had the highest MD event count but only one long-term severe event.

GRAPHICAL ABSTRACT

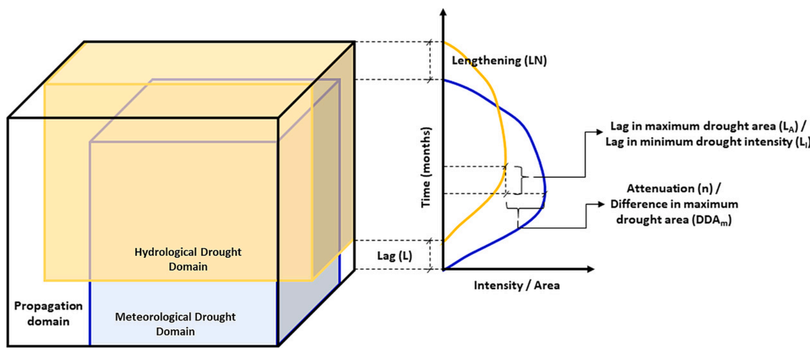

ARTICLE INFO

Editor: Christian Herrera

Keywords:
Meteorological drought
Hydrological droughts
Drought propagation
Cascading droughts
Global drought events
Extreme events

ABSTRACT

An understanding of the spatiotemporal behaviour of Meteorological drought (MD) and Hydrological drought (HD) is crucial for analysing how drought propagation occurs. Here, drought events were treated as three-dimensional grid structures spanning space (latitude and longitude) and time. 31 years (1971–2001) of global MD and HD events were analysed for evidence of propagation, and the most severe 20 MD events explored in detail. From the Inter-Sectoral Impact Model Intercomparison Project (ISIMIP) data archive, precipitation data was used for identifying MD events and an ensemble of simulated runoff from several global hydrological models used for detecting HD events. A technique was developed based on overlapping of the spatial and temporal coverage of MD and HD events, to establish propagation, and to calculate several propagation features. In three dimensions, the transformation from MD to HD was characterised based on delayed instigation, elongated duration, and dampened intensity of the HD event. Additionally, pooling of MD events that resulted in one or multiple branched HD events were identified. Results indicate that minor MD events with short durations and small areas generally do not exhibit propagation. The frequency of HD events with drought duration of 6–12-months is higher than that of MD events with 6–12-month duration. Out of 1740 extreme MD events identified for the 31-year period, 272 events propagated and resulted in 395 extreme HD events. Propagation features for the 20 most severe MD events show substantial variation based on geographical location highlighting the influence of regional climatic and hydrological conditions. This study advances the understanding of global drought propagation mechanisms by addressing key methodological challenges and providing a structured framework for future large-scale drought assessments.

1. Introduction

Droughts are one of the most complex and costly natural disaster with extensive impact on the availability of drinking water, agriculture, and energy production (Wilhite and Glantz, 1985). Droughts can span timescales from a few weeks to decades, and spatial scales from kilometres to continents. Their impacts usually develop slowly and are often indirect, lingering for a long time after the drought itself. By considering usable water, droughts are typically classified into four different types, namely meteorological, agricultural, hydrological, and socioeconomic (Mishra and Singh, 2010). With precipitation being the primary driving force, all these drought types are interlinked. The transitioning of one drought type into another has been widely studied since the proposal. For example, Van Loon (2015) identified that transition from a meteorological drought (MD) to hydrological drought (HD) was associated with sequential anomalies in soil moisture, runoff, and groundwater levels. Studies across regional, continental and global scales have analysed the associations of MD and HD events (e.g. Vicente-Serrano and

López-Moreno, 2005; Dai, 2011; Wong et al., 2013; Haslinger et al., 2014; Xiao et al., 2016; Zhu et al., 2016; Yuan et al., 2017). However, these studies are usually limited to simple time-series assessments of drought area and drought intensity (Vicente-Serrano, 2006; Vidal et al., 2010; Gocic and Trajkovic, 2014; Wang et al., 2015) or focus on area-averaged drought variables (Tallaksen and Stahl, 2014; Ge et al., 2016), which do not provide information on the behaviour of individual drought events.

Few studies have analysed drought development simultaneously in space and time, by tracking drought clusters and analysing their characteristics (Herrera-Estrada et al., 2017). Andreadis et al. (2005) introduced a system to track drought events through time, characterising droughts in higher dimensions. Multiple studies performed similar analysis in other regional areas (Zhan et al., 2016) and globally (Sheffield et al., 2009). Other studies have also explored the algorithm for drought characteristics (such as drought duration, drought area, drought intensity and drought displacement) at country or catchment scales (Vicente-Serrano, 2006; Vidal et al., 2010; Xu et al., 2015; Zhan et al., 2016). Lloyd-Hughes (2012) extended the same approach in three dimensions, analysing similarities and dissimilarities between drought events. Guo et al. (2018) used an improved clustering algorithm for drought identification in Asia, and Diaz et al. (2020) used the same clustering algorithm for drought path identification in India. These studies restricted their analysis to regional scales and hence, a comprehensive study of the spatiotemporal drought characteristics at global scale is needed. In addition, previous studies have been limited to simple time-series assessment of drought area and drought intensity (Vicente-Serrano, 2006; Vidal et al., 2010; Gocic and Trajkovic, 2014; Wang et al., 2015), or analyses that aggregate local drought variables that do not provide information on the behaviour of individual drought events (Tallaksen and Stahl, 2014; Ge et al., 2016).

This study identifies MD and HD events without any boundary restriction to the area. A drought event (spanning in space and time) based approach for drought propagation is rare, and this study aims at providing the first insights into propagation of drought events with a 3D perspective, on a global scale. We propose a new technique, linking MD and HD events to establish propagation, and calculate propagation features. This study details variations in propagation features between drought events and discusses the occurrence and propagation of the 20 most severe drought events from 1971 to 2001 in detail. This research advances our current understanding of drought dynamics, and will be of critical significance to the stakeholders and policy makers.

2. Data and drought indicator

2.1. Datasets

Precipitation and runoff data were extracted from the ISIMIP archive, specifically from phase 2a of the project (ISIMIP2a; Gosling et al., 2017). The precipitation data was derived from the WATer and global CHange (WATCH; Weedon et al., 2011) project, based on the reanalysis dataset ERA-40, and using the bias correction target Global Precipitation Climatology Centre (GPCC) for monthly rainfall and snowfall sums. The WFD climate forcing dataset, covers the period 1901–2001 at a 0.5° x 0.5° spatial resolution.

For HD analysis, an ensemble mean of global daily simulated gridded runoff dataset at a 0.5° x 0.5° spatial resolution from seven global hydrological models (GHMs): DBH (Tang et al., 2007), H08 (Hanasaki et al., 2018), LpJml (Sitch et al., 2003), MATSIRO (Takata et al., 2003), PCR (Wada et al., 2014), VIC (Liang et al., 1994), and WaterGAP2 (Muller Schmied et al., 2016) was used. All the GHMs were run for the period 1971–2001 with the input of climate data from the WFD climate forcing.

All daily values at each grid for both (precipitation and runoff) datasets were aggregated at a monthly time step to avoid influence of variability within a month on the drought estimates.

2.2. Drought indicator

Many drought indices have been proposed to identify and monitor areas under drought but, when it comes to examining and comparing different drought types, standardised indices such as the Standardised Precipitation Index (SPI; McKee et al., 1993) and its variants (Standardised Precipitation Evapotranspiration Index, SPEI; Standardised Soil moisture Anomalies, SMA; Standardised Runoff/Streamflow Index, SRI/SSI; and Standardised Groundwater level Index, SGI) are widely used. Calculation is simple and can be used for different time scales depending on the accumulation period. In addition, these indices do not require substantial data inputs; for example, only precipitation for SPI. One other benefit of using standardised indices is that they represent anomalies from normal in a standardised way, which means that comparisons with other standardised indices for different drought types is possible. In this study, the SPI was used for identifying MD and the SRI for HD identification.

The SPI/SRI for any location is determined based on long-term precipitation/runoff records, preferably >30 years. Monthly precipitation/runoff is aggregated by running over an accumulation period (1, 3, 6, 12, or 24 months). The new series formed is then fitted to a probability distribution (Wu et al., 2018) that subsequently is transformed to a normal distribution such that the mean SPI/SRI is zero (McKee et al., 1993). Here, the “SPEI” package in R (Beguería et al., 2017) was used which allowed us to calculate SPI and SRI during the period 1971–2001 for accumulation periods of 1 and 3 months. Accumulation periods are indicated as SPI-x and SRI-x. For example, SPI-3 and SRI-1 were selected to analyse anomalies in three-monthly precipitation and monthly runoff data, respectively. Any grid cell with a SPI/SRI value less than −1 was considered under meteorological/hydrological drought (Bisht et al., 2019; Liu et al., 2019; Diaz et al., 2020). The error in estimating drought conditions was found to be smallest for extreme conditions (i.e., SPI/SRI values - 2 or less) compared to moderate (SPI/SRI values between −1 and −1.5) and severe conditions (SPI/SRI value between −1.5 and −2) (Kumar et al., 2022). Hence, for this study, we are considering only extreme drought conditions that have SPI/SRI values −2 or less.

3. Methods

3.1. Drought event identification in three dimensions

In this study, a drought event is defined as a three-dimensional structure in space-time. We identify drought events by tracking their spatial extent at each time step. Drought data (gridded SPI or SRI values) can be represented as a set of chronologically arranged maps as a three-dimensional array that spans longitude, latitude, and time (Fig. 1). We identified meteorological and hydrological drought events using the approach of a simple clustering algorithm that incorporated spatial congruity for identification of areas under drought, proposed by Andreadis et al. (2005). The algorithm works on a grid-by-grid basis and uses a 3 × 3 grid-cell moving window for classifying areas into drought clusters. Lloyd-Hughes (2012) extended the same approach from two to three dimensions by using an R×R×R grid moving space-time domain for the search of grids cells under drought. For this study, we used the same approach of identifying and clustering grid cells in the 3D space-time domain.

The algorithm assigns a label to the first grid cell under drought as a drought event, and searches for other grid cells under drought in a moving window of 3 × 3 × 3 grid cells, keeping the already labelled grid cells from the previous search in the centre of the array. It marks all the grid cells found under drought with the same label, and the same procedure is repeated until no grid cell in the 3 × 3 × 3 window is found under drought. This results in 3D structure of grid cells that spans space (longitude X latitude) and time (Fig. 1). We identify these 3D structures as drought events. Drought events are numbered, with MD events given the prefix ‘M’ and HD events the prefix ‘H’.

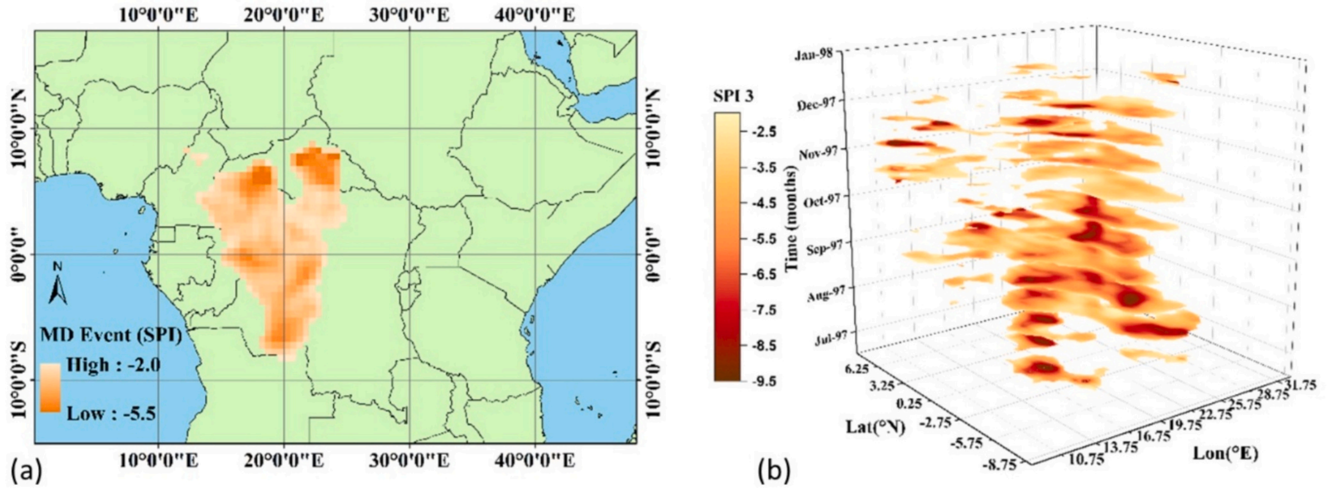

Fig. 1. Spatiotemporal evolution of a meteorological drought event, (a) spatial coverage of the drought event, (b) drought event as 3D cluster of grid cells.

3.2. Calculation of drought characteristics

Fig. 1 shows an example of the 3D grid structure representing a drought event. To analyse and compare 3D droughts events, key drought characteristics must be determined and calculated. For this study, we define the drought characteristics as follows:

a) Onset time (T_o) and termination time (T_t): Traditionally refers to the beginning and end of a drought event in a given area. In 3D space, drought events consist of multiple connected grid cells that can have different start and end times. Therefore, the onset and termination time refers to the earliest initial and latest terminal time of all connected grid cells that constitutes the drought event.
b) Drought duration (T): Refers to the time span (in months), between T_o and T_t of a drought event.
c) Drought area (DA): Given the 3D structure of drought events, the drought area may vary with time. Therefore, here drought area refers to the area under drought (in number of grid cells) at each time steps during a drought event.
d) Maximum drought area (DA_m): is the maximum DA (in number of grid cells) for the time span of a drought event.
e) Drought intensity (DI): represents the mean SPI/SRI value over the DA at any given time step of the drought event.
f) Minimum drought intensity (DI_m): is the minimum of DI for the time span of a drought event.

3.3. Drought propagation in three dimensions

HD events are inherently the response of MD events and are connected. To understand this relationship, we propose a new method to characterise drought propagation, which takes into account the interrelatedness of MD and HD events. The term 'drought propagation' can sometimes refer to the spatial migration of a drought event due to the atmospheric transport of anomalously warm and dry air (Joseph et al., 2009; Diaz et al., 2020). In this paper, drought propagation refers to the transformation between MD and HD events. Fig. 2 presents a flowchart of the algorithm used for defining the propagation phenomenon. The algorithm uses a domain-based approach by defining the propagation domain for each MD event, entailing the steps listed below.

Step 1: Defining the meteorological drought domain

For a MD event, we calculated its spatiotemporal range by establishing its 3D extent in the meteorological dataset defined as the MD domain. The MD domain represents the maximal range in space-time for a given MD event (Fig. 3(a)).

Step 2: Defining hydrological domain

After defining the initial MD domain, we identified all the MD and HD events present in the MD domain using meteorological and hydrological datasets respectively. For both the MD and HD events in the MD domain in their respective datasets, the spatiotemporal range of each event is calculated separately. Any MD or HD event that had >70 % of its grid cells in the initial MD domain were considered to be part of the propagation process (Fig. 3(b)), but were also studied separately for propagation. These additional drought events (ADE) and HD events were then used to update the MD domain to its larger total extent (updated MD domain) and to calculate the HD domain respectively. The HD domain therefore represents the range in space-time which fully contains all the HD events identified in the MD domain.

Step 3: Establishing propagation domain

Based on the MD domain and HD domain, a new domain is defined in such a way that it encompasses both the domains; termed the propagation domain (PR domain). It represents the space-time range in which the transformation of MD events to HD events can be observed (Fig. 3 (c)).

3.4. Calculation of propagation features

For the propagation analysis, we only considered MD events longer than 3 months and having a spatial extent of >4 grid cells with longitudinal and latitudinal range exceeding 2 grid cells each (further explained in Section 3.5). To analyse the transition of MDs into HDs (i.e. drought propagation) multiple features were calculated, termed propagation features. This includes pooling of drought events, lengthening, attenuation, difference in spatial extent and lag. Calculating these features is an attempt to quantify the complexity of drought propagation. Propagation features (defined below) were calculated based on the characteristics of MDs and HDs in the defined PR domain, as shown in Fig. 4.

a) Lag (L) refers to the time gap (in months) between the onset time (T_o) of the earliest MD and HD event. Positive values indicate that the onset of HD events is later than the MD events.
b) Lengthening (LN) is the time (in months) of HD events after the termination time (T_t) of MD events. Positive values indicate that the termination of HD events is later than the MD events.

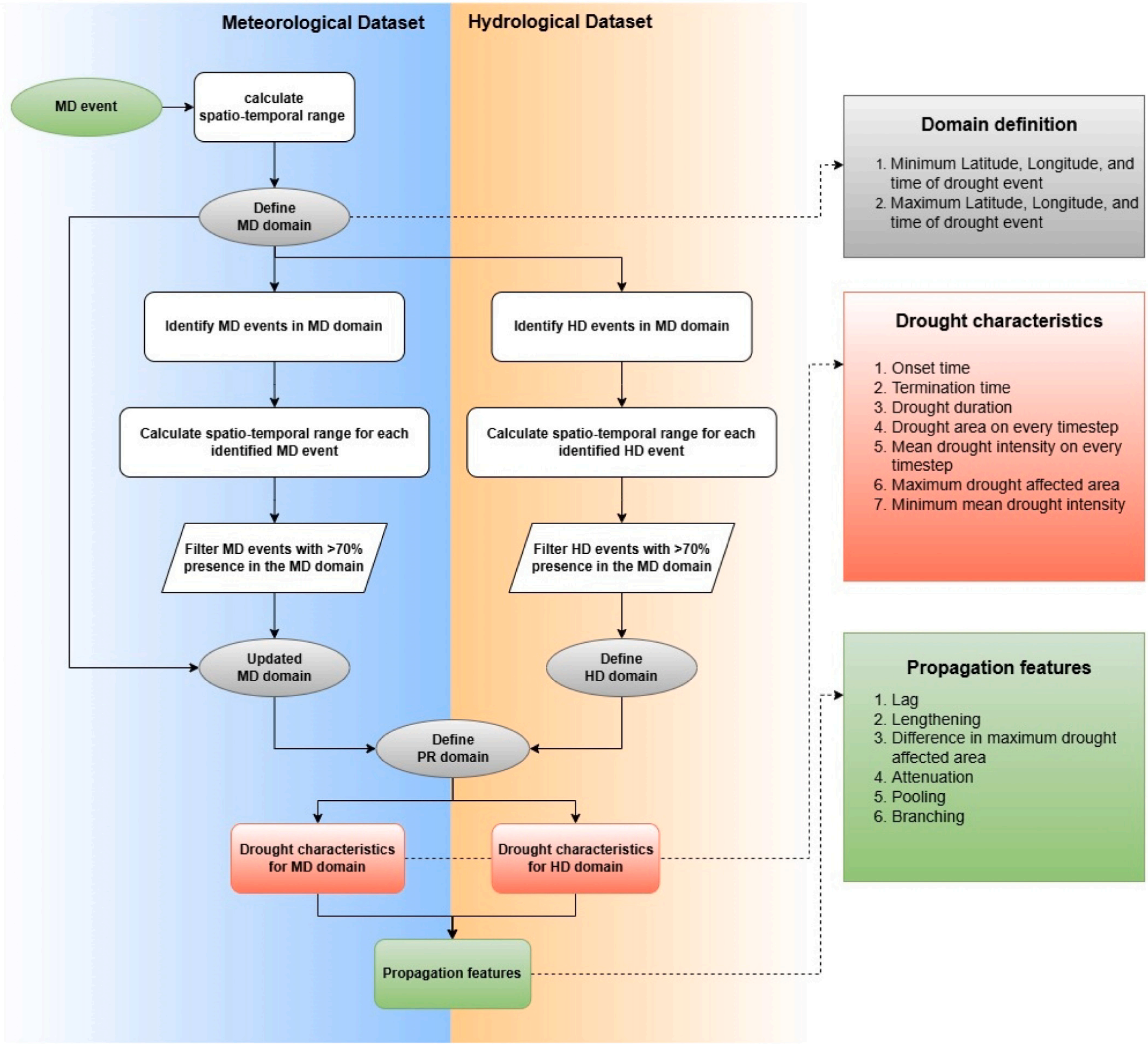

Fig. 2. Flow diagram showing the sequence for calculating 3D drought extents and extraction of key drought characteristics and propagation features.

c) Difference in maximum drought area (DDA_m) is the difference in DA_m of MD and HD events, quantifying the variation in maximum spatial extent (in number of grid cells) due to propagation. Positive values show greater spatial extent of MD events in comparison to HD events.
d) Attenuation (n) refers to the difference in magnitude (in SPI/SRI value) of the DI_m of the HD event compared to MD event due to propagation. Negative values indicate a reduction in DI_m i.e. HD event being less intense than the MD event.

e) Pooling (p) is the total number of MD events (i.e. the ADE's and initial MD event) that combine into prolonged HD events.
f) Branching (b) is the total number of HD events resulting from the ADEs and MD event.

3.5. *Identification of most severe MD events*

Initially for the 31-year period (1971–2001) 25989 MD and 35,307 HD structures were identified. Temporal and spatial filters were applied for the identification of drought events of global significance. Only drought structures having a time length >3-months (temporal filter) and a spatial range >4 grid cells (spatial filter) were identified as drought events. After filtering, 1740 and 1493, MD and HD events respectively were identified. This shows that there were more globally significant MD events than HD events.

From the 1740 MD events, we identified the 20 most severe MD events for the period 1971–2001 (Table 1). Severe events were identified in this study based on three drought characteristics: T, DA_m and DI_m. All the 1740 MD events were separately ranked on each drought characteristic and the sum of ranks was calculated. The sum of ranks determined the place of a MD event in the collective ranking of all events. Higher values represented higher ranks and hence less severe drought events, while lower values representing more severe events. The top 20 MD events were considered for more detailed propagation explanation.

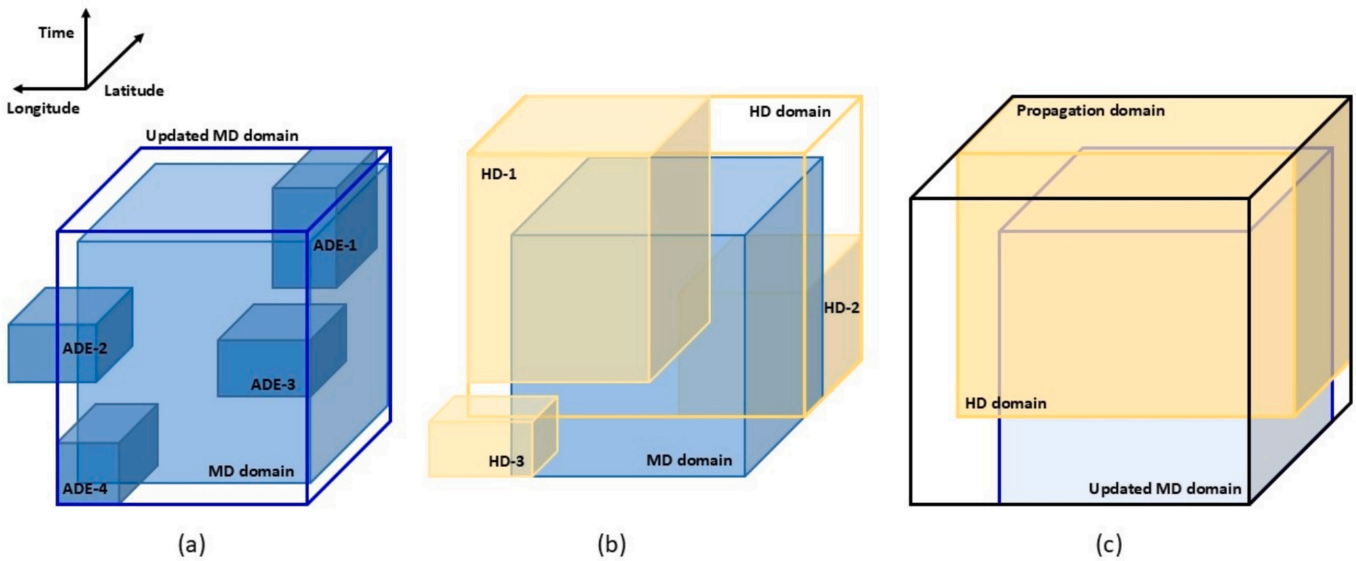

Fig. 3. Conceptual diagram showing role of (a) meteorological drought and (b) hydrological drought domain in defining (c) propagation domain; Additional Drought Events (ADE-x) and hydrological drought events (HD-x) having >70 % of their grids overlapping MD domain in their respective datasets i.e. ADE-1, ADE-2 and ADE-3 in meteorological dataset, and HD-1 and HD-2 in hydrological dataset were used to update MD domain and HD domain.

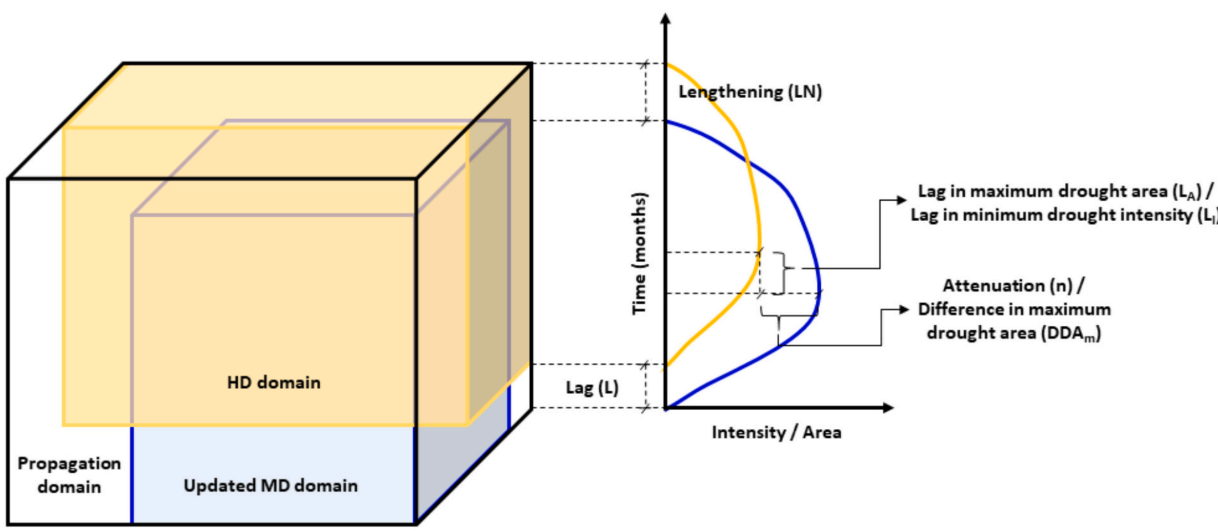

Fig. 4. Conceptual diagram showing updated meteorological drought (MD), hydrological drought (HD) and propagation domains along with graphical representation of propagation features.

4. Results

4.1. All drought events globally

A decline in the difference between the number of MD and HD events was found as T increased. Fig. 5 shows the frequency distribution of MD and HD events based on T. Drought events were categorised based on T, with events having T <6-months, between 6 and 12-months, and >12-months (i.e. short-, medium- and long-term drought events). The number of HD events was greater than MD events for medium-term events whereas MD events were more frequent than HD events for short- and long-term event categories. Average DA_m increases with T for both MD and HD events (Fig. 6). Average DA_m in all three categories was greater for MD than HD events, showing MD tended to have greater spatial coverage than HD events in each category. On average, DA_m for HD events was <50 % of MD events for short- and medium-term drought events while approximately 30 % for long-term events.

4.2. Drought propagation

Of the 1740 MD events identified using the methodology explained in Section 3.1, 272 MD events propagated from MD to HD events. Short- and medium- term events showed less tendency towards propagation than the long-term events. Out of 49 long-term events, 41 showed propagation i.e. ~84 %, while for medium- and short-term events the number of MD events showing propagation was ~30 % (175 of 574) and 5.5 % (62 of 1117), respectively.

4.2.1. Propagation features of all drought events

For each propagated MD event, a PR domain was defined based on MD and HD domains as explained in Section 3.3, and propagation features were calculated (Section 3.4), an example is shown in Fig. 7. Drought events undergoing propagation experience an initiation lag, lengthened duration, and attenuated drought intensity. Of the 272 propagated MD events, 53 % had a positive lag, with average duration of

Table 1
Drought characteristics for most severe MD events.

	Meteorological drought (*MD*) ID	Start month	Drought duration (*T*)	Max drought area (DA_m)	Minimum drought intensity (DI_m)	Location	Reported studies
1	M-894	Mar-1988	10	81	−5.4	Africa	(Masih et al., 2014)
2	M-1125	Aug-1993	13	631	−3.5	Africa	(Ndehedehe et al., 2019); (Sori et al., 2021); (Masih et al., 2014)
3	M-1481	Jul-1997	13	456	−3.4	Africa	(Ndehedehe et al., 2019); (Masih et al., 2014)
4	M-1571	Oct-1998	10	315	−3.2	Africa	(Masih et al., 2014)
5	M-11	Jan-1971	10	133	−3.4	Asia	(Nasrati, 2018); (Rathjens, 1975)
6	M-418	Jul-1979	12	568	−3.1	Asia	(Wattanakij et al., 2006); (Limsakul et al., 2011)
7	M-502	Jul-1981	9	288	−3.2	Asia	(Utkuzova et al., 2015); (Glazovsky, 2009)
8	M-1277	Apr-1994	9	140	−4.0	Asia	(Saji et al., 1999); (Field et al., 2004); (Hatmoko et al., 2015)
9	M-1433	Dec-1996	15	168	−3.8	Asia	(Saji et al., 1999); (Field et al., 2004); (Hatmoko et al., 2015)
10	M-1495	Aug-1997	11	137	−3.4	Asia	(Slik, 2004); (Keil et al., 2008); (Van Nieuwstadt and Sheil, 2005)
11	M-1588	Jan-1999	10	258	−3.6	Asia	(Dahal et al., 2016); (Sigdel and Ikeda, 2010); (Das et al., 2016)
12	M-252	Dec-1975	16	690	−3.1	Europe	(Rodda and Marsh, 2011); (Spinoni et al., 2015); (Parry et al., 2012); (Tanguy et al., 2021)
13	M-674	Mar-1984	11	379	−3.9	North America	(Nicklen et al., 2019); (Csank et al., 2016); (Verbyla, 2008); (Barber et al., 2000)
14	M-867	Aug-1987	13	496	−3.1	North America	(Shukla et al., 2011); (Lettenmaier et al., 1990)
15	M-931	Mar-1989	8	197	−3.9	North America	(Xiao and Zhuang, 2007)
16	M-376	Jun-1978	20	114	−3.5	South America	(Loaiza Cerón et al., 2020); (Mortensen et al., 2018)
17	M-597	Jan-1983	32	179	−6.9	South America	(Mortensen et al., 2018); (Vicente-Serrano et al., 2015); (Cavledes, 1985)
18	M-637	Jul-1983	10	74	−4.7	South America	(Alencar et al., 2015); (Li et al., 2008); (Saatchi et al., 2013)
19	M-638	May-1984	25	289	−3.5	South America	(Loaiza Cerón et al., 2020); (Mortensen et al., 2018)
20	M-882	Oct-1987	19	596	−3.4	South America	(Mortensen et al., 2018); (Vicente-Serrano et al., 2015)

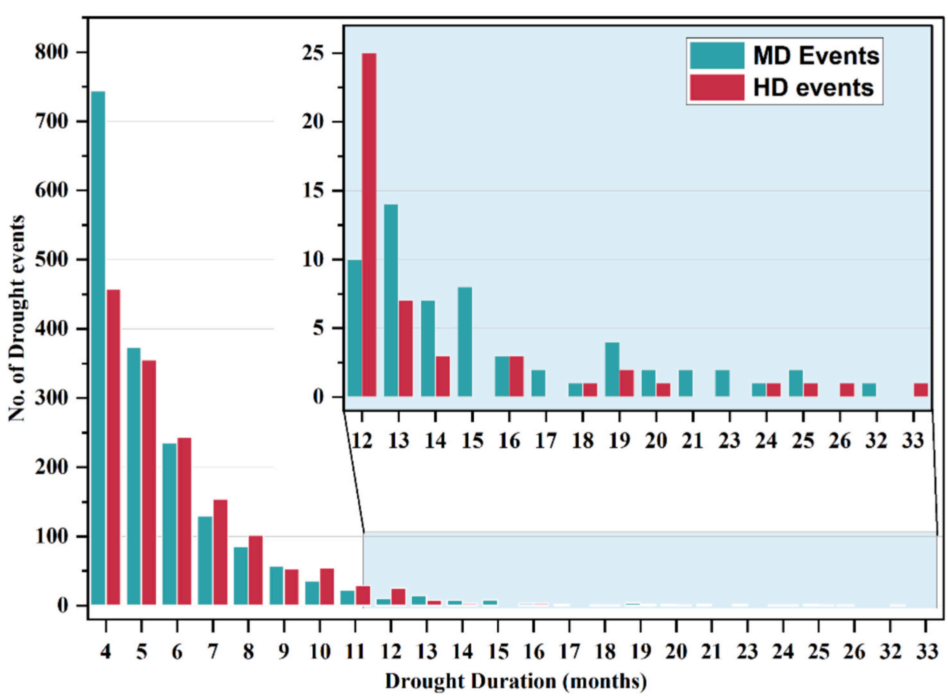

Fig. 5. Frequency distribution of MD and HD events based on duration of drought events.

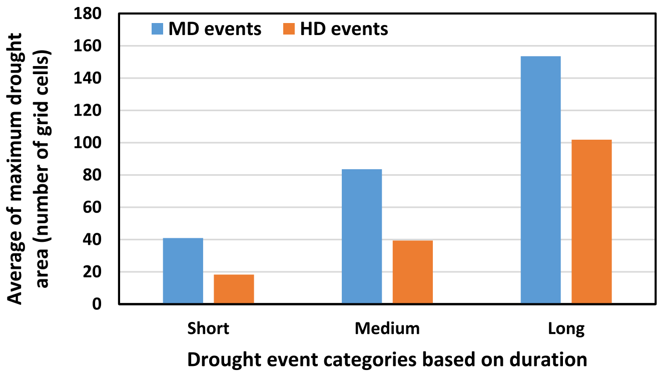

Fig. 6. Average maximum drought area (average DA_m) for MD and HD under three drought event categories (short-, medium-, and long-term events).

3-months. No lag was observed in 32 % of droughts and a negative lag was observed in the remaining 15 %. Lengthening (*LN*) was observed for 33 % of propagated MD events with an average duration of 2 months, 43 % showed negative *LN* (i.e. termination of HD events before the termination of MD event); with no *LN* observed in the remaining 22 %.

As a sign of propagation, we also observed attenuated DI_m (*n*) for 80 % of the total propagated MD events. In addition to the *L*, *LN*, and *n*, we also observed a difference in DA_m (DDA_m) as an effect of propagation. 88 % of propagated MD events showed a reduction in spatial coverage after propagation; DA_m of MD events reduced by >50 % in 158 propagated MD events. In contrast, 9 % of propagated MD events experienced expansion of DA_m after propagation, averaging a 30 % area increase.

4.2.2. Pooling and branching of all drought events

The total number of MD events that join is the pooling value; for example, a pooling value (*p*) of 2 indicates 2 MD events combining for propagation. The equivalent branching value (*b*) indicates MD events causing multiple HD events, so a value *b* of 2 indicates that MD event/s caused 2 HD events. 30 MD events showed pooling; *p* varied from 2 to 9, showing that the additional MD event count ranges from 1 to 8 MD events (Fig. 8(a)). 58 propagated MD events branched into 2 or more HD events with *b* ranging from 2 to 10 (Fig. 8(b)). From 30 propagated MD events showing pooling, 80 % (24 in 30) also showed branching, indicating higher affinity towards branching if MD event also exhibit pooling. The majority of the propagated MD events did not show either pooling or branching.

4.2.3. Propagation of the 20 most severe MD events

The most severe MD events were distributed globally (Table 1). None of the 20 events were restricted to a single country. *T* and DA_m for these events varied substantially from 8 to 32 months and from 74 to 690 grid cells, respectively. The MD event having shortest *T* was from North America (8 months) and longest from South America (32 months). 9 out of 20 MD events lasted for more than a year i.e. long-term events, while the remaining other 11 MD events were medium-term events. Asia, despite having most of the top 20 events, only had 1 MD event in the long-term category. The MD event that covered the largest area was from Europe (Fig. 7(b)). The most severe event in terms of *DI* was from South America with DI_m of −6.9 (SPI).

All the top 20 most severe MD events propagated, except for 1 (M-867). M-867 was a 13-month long event in western North America with a DA_m of 496 grid cells. Of the 19 MD events showing propagation, 14 had a positive lag ($L = 3$ months), while 4 showed no lag and 1 had a negative lag of 1 month (Table 2). 8 events resulted in lengthened HD events, no LN was observed for 5 MD events and there was a negative *LN* for the remaining 6 events. Attenuated DI_m and reduced DA_m was also observed for all 20 most severe events after propagation except for 1 event from Africa (M-1571) showing increased DI_m. The reduction in DA_m varied from 16 to 97 %, skewed towards MD events with spatial extent >100 grid cells. In addition, out of the 19 propagated events, 8 exhibited pooling and 9 showed branching, while 7 showed both showing that events with pooling have higher affinity towards branching.

4.3. Consistency with other studies

Many other studies have analysed large scale droughts, either as individual events or from a regional climatological perspective, and their impacts are generally well documented. In the following section, the occurrences of the most severe MD events are qualitatively compared (Table 1) and related HD events with some of these studies.

4.3.1. Africa

The 4 African MD events in the top 20 occurred between 1988 and 1998, covering the majority of the mid- and north-western countries, particularly around the Congo River basin, including the Democratic Republic of Congo, Angola, Zambia, and Tanzania. Multiple studies report individual drought events during late 1980s and mid-1990s from these areas. The Congo basin was characterised to have persistent and severe multiyear droughts during the end of last century (1991–2001); for example, Sori et al. (2021) reported 53 MD episodes that affected Congo basin during 1981–2018. The impacts of these drought events were extensive, affecting >40 % of the basin during 1994–2006 (Ndehedehe et al., 2019). Lower contribution of moisture by Congo basin (Sori et al., 2021) and Pacific El Niño–Southern Oscillation (ENSO) and other multiscale ocean-atmosphere phenomena influences large deviations in precipitation and impacts hydro-climatic extremes (Ndehedehe et al., 2019).

4.3.2. Asia

All 7 events in Asia were widely distributed across the Asian continent i.e. 4 events in Indonesia and Thailand, 1 in Afghanistan, 1 in Nepal, Bangladesh and north-eastern part of India, and 1 in the lower Asian area of Russia. All events were medium-term except for 1 long-term event (M-1433) from Indonesia.

The 4 MD events (M-418, M-1277, M-1433 and M-1495) we identified in parts of Indonesia and Thailand occurred during late 1970s and late 1990s. Limsakul et al. (2011) identified an abrupt drying during the mid-1970s in Thailand and Wattanakij et al. (2006) reported the year 1979 as one of the driest on record based on daily rainfall records. 1994 and 1997 in Indonesia have been analysed extensively presenting dipole mode event in the tropical Indian Ocean (Saji et al., 1999), developing early warning system for droughts (Hatmoko et al., 2015) and predicting haze events based on droughts (Field et al., 2004). Keil et al. (2008) reports the year 1997 as one of the most severe drought experienced. Slik (2004) investigated effects of 1997/98 drought on tree mortality while Van Nieuwstadt and Sheil (2005) reported stem mortalities to be most severe due 1997 drought event.

Event M-502 in Russia from 1981 to 82 was reported by Utkuzova et al. (2015). According to Glazovsky (2009), 47.5 % of the Russia land falls under climatic zones where desertification and droughts are likely to occur. For MD event M-1588 covering Bangladesh, Nepal and neighbouring parts of India in 1999, we found multiple studies reporting the same event at regional scale. Dahal et al. (2016), Sigdel and Ikeda (2010) reported 1999 as deficient in winter rainfall and one of a number of dry occurrences based on monthly mean precipitation data. In addition they found a significant correlation between winter SPI-3 values and the Indian Ocean Dipole Mode Index. Das et al. (2016) reported a drought event in 1999 over north and north-eastern parts of India, and Rahman and Lateh (2016) identify 1999 as the worst drought year for Bangladesh. Nasrati (2018) and Rathjens (1975) reported that in 1970 and 1972 Afghanistan received below normal precipitation which caused drought, crop failure, loss of livestock, and in some regions even famine.

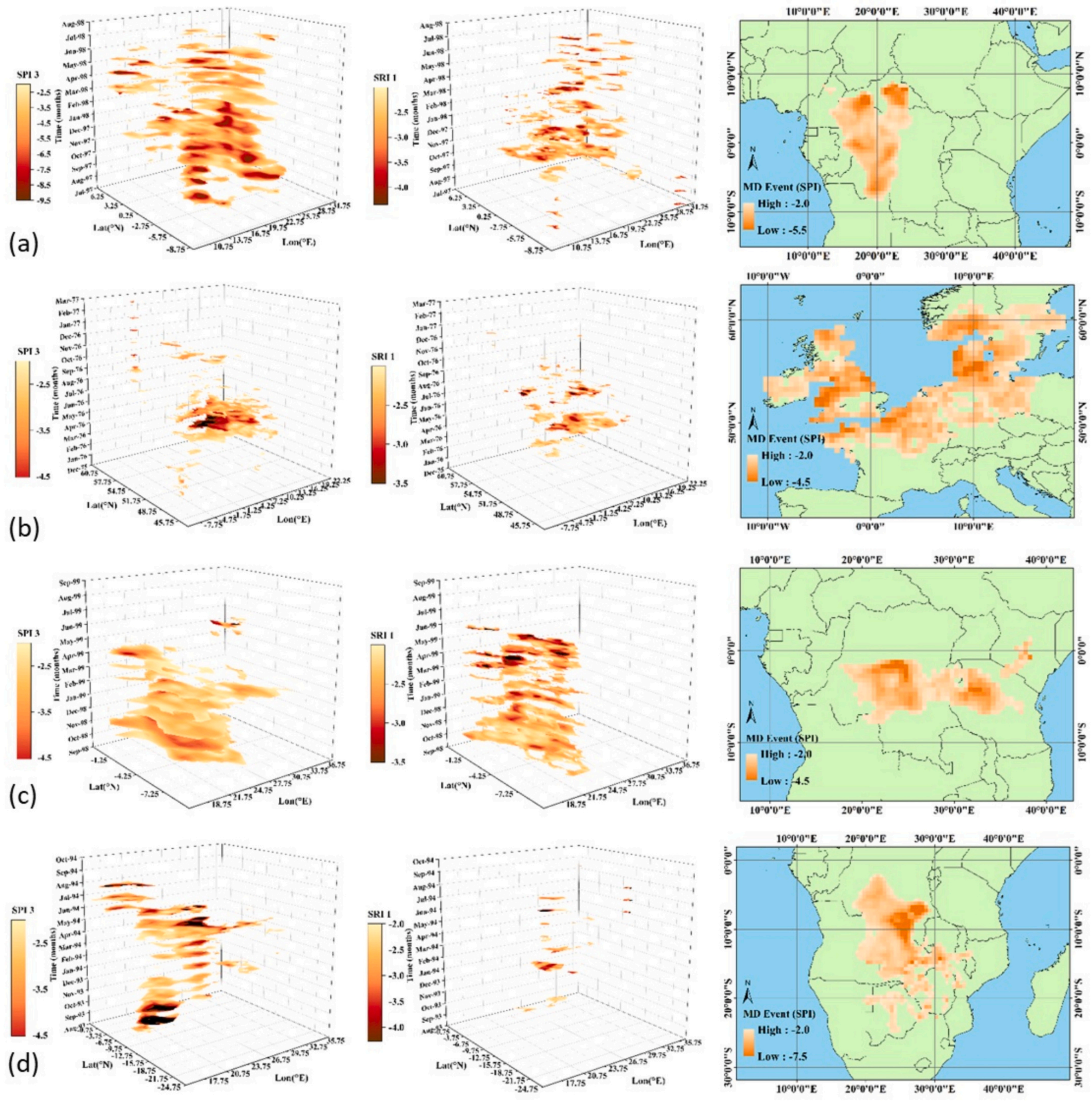

Fig. 7. Propagation of drought events from MD to HD with its spatial coverage in each panel, showing propagation features ‘pooling’ and ‘branching’: (a) M-1481 (with no pooling and branching), (b) M-252 (with no pooling but branching), (c) M-1571 (with pooling but no branching), and (d) M-1125 (with pooling and branching).

4.3.3. *Europe*

Only 1 MD drought event (M-252) was identified in Europe, which propagated into 4 different HD events. The MD event was 16 months long from 1975 to 77 and covered western European countries including United Kingdom, Belgium, Netherlands, Denmark, with parts of France, Germany, Czech and Norway, detailed by Parry et al. (2012) and Spinoni et al. (2015). Rodda and Marsh (2011) compiled a comprehensive report on the drought of 1975–76 explaining its occurrence and expansion from a UK perspective. Generalising broadly, the report states that the drought developed through the late spring of 1975 and intensified during late summer of 1976.

4.3.4. *North America*

All 3 North American MD events were from northern regions covering Alaska, parts of Canada, and Washington State, USA. No study directly reported the Alaska drought event from 1984 (M-674); however, Verbyla (2008) reported a significant decreasing trend in normalised difference vegetation Index (NDVI) among interior boreal forest of Alaska, while Csank et al. (2016) found their results consistent with studies of carbon starvation because of either drought or insect attack. Barber et al. (2000) registered severe, prolonged, and unprecedented warmth and dryness in the 1980s and 1990s for Alaska. The Washington drought of 1987 (M-867) is a well-documented drought event

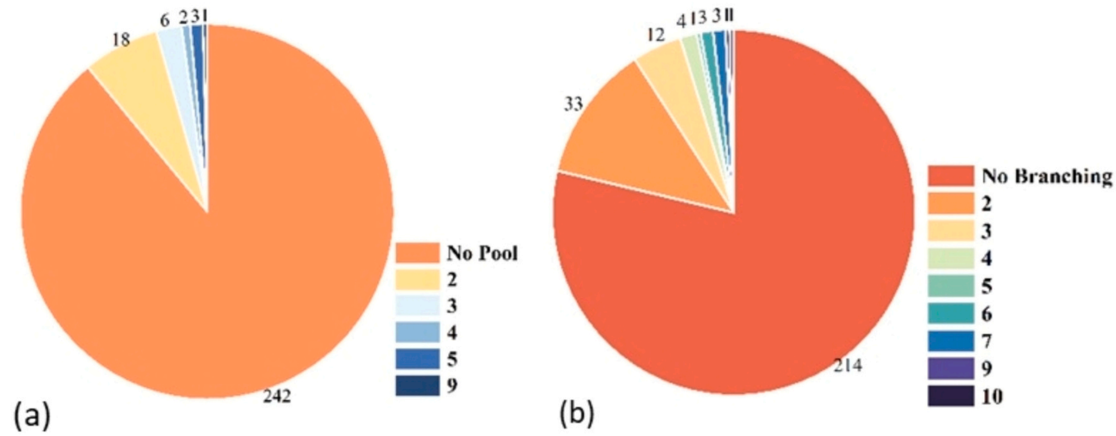

Fig. 8. Propagated MD events showing number of events exhibiting (a) pooling, and (b) branching.

(Lettenmaier et al., 1990; Shukla et al., 2011) and the only MD event among the most severe that did not show propagation. The 1987 drought caused severe water shortages in many areas of Washington, and was termed as one of the costliest U.S. droughts by Riebsame et al. (2019). The drought of 1989 (M-931) covered parts of Alaska and western Canada, and resulted in fire activities in Canadian and Alaskan forests. Xiao and Zhuang (2007) reported that during large fire of 1989, about 57 % and 84 %, of Canada and Alaska forest region, respectively were drought affected.

4.3.5. South America

Five MD events from South America were identified, which resulted in 18 HD events. All the identified MD events were long-term events except 1 (M-637). The MD events mostly covered northwestern parts of South America including Peru, Colombia, Bolivia, Ecuador, Brazil, and Venezuela. Researchers have reported increasing drought trends in southern parts of the Amazon basin (Li et al., 2008; Saatchi et al., 2013), and drought events resulting in forest fires (Alencar et al., 2015) for 1970–2000. Loaiza Cerón et al. (2020) identified annual drought events in years 1978 (M-376) and 1984 (M-638), reported by >90 % and 50 % of meteorological stations in Colombia, respectively. Cesar (1985) reported an emergency and institutional crisis in Peru due to the 1983 El Nino drought. Lower Peru and Bolivian droughts of 1983 (M-597) and 1987 (M-882) were recorded by Vicente-Serrano et al. (2015) while studying spatiotemporal variability of droughts in Bolivia during 1955–2012.

5. Discussion

5.1. Factors governing drought propagation

272 MD events propagated from a total of 1740 MD events, indicating that propagation of drought events from MD to HD is a rare phenomenon. In addition, long-term events showed much higher tendency towards propagation than short- and medium-term events due to increased water deficit over the period. Long-term events are more frequent in tropics and European temperate zone compared to rest of the world. The tropics are generally characterised by high seasonal variability and delayed recovery which is why the majority of these long-term events showing propagation belong to tropical rainforest of Africa, Asia and South America.

Complexity of drought propagation arises from its dependence not only on atmospheric parameters but also on hydrological processes including water storage and stream flows (Mishra and Singh, 2010). Precipitation and temperature are the two main atmospheric parameters that govern hydrological conditions in any area. Both precipitation and temperature anomalies can be associated with large-scale ocean patterns like ENSO, NAO, and sea surface temperatures (Kingston et al., 2013, 2015). During extreme drought (MD) conditions, reduced soil moisture affects evapotranspiration, which in conjugation with precipitation deficits helps in sustaining drought conditions in different water resources that leads to HD. Hence, drought propagation characterised by propagation features (Section 3.4) is governed by not only climatic factors but also by catchment characteristics. Lag, lengthening and attenuation are dependent on catchment characteristics while, pooling and branching, on both catchment characteristics and climatic factors (van Lanen et al., 2004; van Loon, 2013).

5.2. Dependence on climatic factors

HD develops differently for stable climates when compared to climates with strong seasonality (Van Loon, 2015). This results in variation in propagation features between different climate regions. Various researchers have examined the dependency of drought characteristics on climatic factors, while dependency of propagation features is much less explored. In areas with stable climatic conditions, lower than normal precipitation is the main governing factor responsible for drought development while for areas with a seasonal climate, associated hydrological processes play a vital role in the development of summer or winter droughts i.e. short- or medium-term droughts. These drought events in absence of recovery results in long-term events and/or propagation. On the other hand, for regions with strong seasonality, MD events are generally short- and medium-term, and seasonality in climate often helps in recovery, leading to an early termination of HD events after propagation reflected as negative lengthening.

For the European temperate zone, persistence of lower than normal precipitation can lead to long-term drought events while in the tropics, inadequate or obstructed recovery builds up longer drought events that can result in propagation. The M-252 drought event from 1975 affecting the UK and northern Europe was the result of a series of dry winters leading to a multiyear HD (Peters et al., 2006). For parts of Alaska, Canada and Russia, below-zero temperatures, frozen soil and accumulated snow often results in decreased streamflow throughout winter (Huntington and Niswonger, 2012; Sheffield and Wood, 2012). However, for 'Wet-to-dry-season drought' (Van Loon and Van Lanen, 2012), where rainfall deficit of wet season continued into the dry season with very less recovery, resulting in drought events such as M-376, M-597, etc. (South America), M-894, M-1125, etc. (Africa), and M-11, M-1588, etc. (Asia).

In addition, for some parts of Asia and Africa where dry and wet seasons alternate due to large-scale oceanic patterns, and climate is monsoonal, experiencing dryer conditions is normal. Hence, such dry conditions are not normally identified as drought, which is the main reason behind the smaller number of reported drought events from these

Table 2
Events that propagated from most severe MD events and their propagation features.

Location	Meteorological drought event	Additional drought event	Hydrological drought events	Drought duration		Lag	Lengthening	MD drought area	Percentage difference in drought area	Attenuation	Pooling	Branching
	MD	*ADE*	HD	MD	HD	*L*	*LN*	DA_m	DDA_m	*n*	*P*	*b*
	Event label	Event label	Event label	Months	Months	Months	Months	Number of grids cells	Percent	SPI/SRI value	Event count	Event count
Africa	M-894	–	H-784	10	11	2	3	81	48	−2.5	–	–
	M-1125	M-1233, M-1239, M-1275	H-1036, H-1082, H-1085	13	14	1	2	639	70	−0.7	4	3
	M-1481	–	H-1236	13	14	–	1	456	39	−0.8	–	–
	M-1571	M-1568, M-1606	H-1331	13	12	1	–	339	36	0.6	3	–
Asia	M-11	M-38	H-11, H-17, H-26, H-28, H-29, H-31	10	10	–	–	133	16	−0.8	2	6
	M − 418	–	H-388	12	5	3	-4	568	97	−0.7	–	–
	M-502	–	H-466	9	4	4	−1	288	95	−0.7	–	–
	M-1277	–	H-1083	9	8	1	–	140	58	−1.3	–	–
	M − 1433	–	H-1238	15	7	7	-1	168	30	−1.1	–	–
	M-1495	–	H-1244, H-1289, H-1299	11	13	–	2	137	48	−0.3	–	3
	M-1588	M-1611	H-1356, H-1371	10	12	1	3	258	84	−0.4	2	2
Europe	M-252	–	H-246, H-245, H-244, H-284	16	13	3	–	690	48	−0.6	–	4
North America	M-674	–	H-570	11	12	2	3	379	62	−0.8	–	–
	M-931	–	H-814	8	9	−1	–	197	95	−1.5	–	–
South America	M-376	M-371	H-330, H-353, H-370	21	19	1	−1	114	57	−0.6	2	3
	M-597	M-637	H-512, H-522, H-524, H-554, H-572	32	33	–	1	179	74	−2.4	2	5
	M-637	–	H-554	10	5	4	−1	74	39	−1.7	–	–
	M-638	M-681, M-684, M-707, M-712	H-571, H-579, H-585, H-627, H-631, H-670	26	27	1	2	295	74	−0.6	5	6
	M-882	M-883, M-873, M-874, M-890, M-897, M-903, M-912, M-913	H-780, H-796, H-800	24	13	6	−5	617	94	−0.5	9	3

areas. In general, delayed monsoon or partial/complete failure of monsoon is reported as drought (Flatau et al., 2003; Schewe and Levermann, 2012).

5.3. Dependence on catchment characteristics

Hydrological processes and catchment characteristics shows intermixed mechanisms which influence drought propagation (van Lanen et al., 2004). The catchments response time towards precipitation deficit is an important factor that governs propagation features. It can be used as a proxy for a combination of catchment characteristics indicative of water retention or storage. Propagation features like lag, lengthening and attenuation heavily dependent on catchment characteristics and hence on catchment response time. Slow responding catchments show long time lag between MD and HD events, such as drought event M-637 covering parts of Amazon catchment from South America, and M-252 from European region.

One important catchment characteristic that strongly influences drought propagation is the storage capacity of a catchment (van Lanen et al., 2004; Brutsaert, 2005). The amount of water retained or stored by soil in the form of soil moisture depends largely on soil type, organic matter present in soil, and the area of the catchment which in turn significantly affects flow in streams (Eng and Milly, 2007). Anomalies in storage capacity along with climatic anomalies such as evapotranspiration anomalies in central and western European catchments have resulted in prolonged HD events (Teuling et al., 2013). Aquifers are also a prevalent source of storage that has a strong influence on drought development and recovery (Aeschbach-Hertig and Gleeson, 2012; Gleeson et al., 2014). For regions with porous and complex aquifers, drought propagation is typically catchment-controlled because surface water flows are largely determined by groundwater level and connectivity, and are less responsive to precipitation over short- to medium-timescales ($<$ 12 months) (Stoelzle et al., 2014). Therefore, these areas are associated with longer lag times between precipitation deficits and drought conditions, such as for drought events M-418, M-502, and M-1433 in Asia. In contrast, regions with fractured aquifers typically have shorter response times, showing almost no lag or lengthening, as observed for drought events M-1481, M-1495 and M-597.

5.4. Conditions affecting pooling and branching of drought events

Pooling and branching of drought events were even rarer than propagation. Unlike lag, lengthening and attenuation which are more catchment controlled, pooling and branching both are governed by the interplay of both climatic factors as well as catchment characteristics. The occurrence of both pooling and branching can be easily identified by mapping the drought affected regions. The spatial coverage of a drought events ranges from catchment to continental scales, however depending on the drought type spatial coverage may vary. MD events, due to their dependence on large-scale atmospheric drivers, typically covers large areas (Fig. 6) in contrast to the comparatively smaller and sparser spatial pattern of HD events that dependent on local catchment characteristics. Large catchments with a range of elevation, show high spatial variability in temperature and precipitation, leading to reduced spatial development of HD events (Van Loon, 2015). For the drought events M-882, M-931, M-1588, M-502, and M-418 the elevation differences in topology have led to scattered HD events in parts of central South America, southwest Canada, northeast India, southeast Asia and Siberian Russia respectively. In addition, as stated by Hannaford et al. (2011), we found that MD events in European region were found to be more coherent than HD events. For instance, drought event M-252 from parts of UK and Europe was unified while it branched out into several smaller HD events after propagation. This disjointment in spatial coverage of HD events is the main reason behind skewed synchronicity of MD and HD events (Lloyd-Hughes, 2012; Verdon-Kidd and Kiem, 2014). Moreover, catchments from tropical part of Africa and South America also have climatic conditions majorly driven by ENSO or other multiscale ocean-atmosphere phenomena (Masih et al., 2014; Ndehedehe et al., 2019), and are lager in size covering several thousand square kilometres in area with huge spatial variability which can be attributed to pooling of drought events from these areas.

6. Conclusion

This study describes the spatio-temporal characteristics of global drought events and their propagation from meteorological drought (MD) to hydrological drought (HD) events over the period 1971–2001. Drought events were defined based on precipitation and ensemble runoff datasets in the form of three-dimensional grid clusters spanning space (latitude and longitude) and time. We analysed drought events based on duration, intensity, and area, and identified the 20 most severe MD events globally. The study proposes a new technique based on overlapping of spatial and temporal coverage of MD and HD events, to establish propagation, and calculated several propagation features.

Using a 3D clustering method, we identified 1740 and 1493, MD and HD events respectively. Out of 1740 MD events, 272 events propagated into 395 HD events, indicating that propagation is rare. Most of the MD events, mainly constituting short- and medium-term events did not exhibit propagation while majority of the long-term MD events propagated, showing greater tendency of long-term MD events towards propagation. The majority of the propagated MD events showed positive lag, negative lengthening, attenuated intensity, and reduced spatial coverage indicating that MD events after propagation are resulting in one or more HD events of smaller size. Although all the propagated MD events did not show either pooling or branching, the majority of the propagated MD events that showed pooling also showed branching, indicative of higher affinity towards branching if a MD event also exhibits pooling.

All the 20 most severe events identified were consistent with those reported in scientific and popular literature, and showed propagation except one MD event from Africa. Asia, despite having the highest number of MD events out of the most severe events, the region only had one long-term MD event. Consistent with the majority of propagated MD events, majority of the most severe MD events showed positive lag. However, in contrast, the majority of the most severe MD events showed positive lengthening which was inconsistent with the majority of all propagated MD events. Drought events from Africa and South America showed higher tendency of pooling and branching due to favourable climatic and catchment characteristics.

CRediT authorship contribution statement

Amit Kumar: Writing – review & editing, Writing – original draft, Visualization, Validation, Methodology, Investigation, Formal analysis, Data curation, Conceptualization. **Simon N. Gosling:** Writing – review & editing, Conceptualization. **Matthew F. Johnson:** Writing – review & editing, Conceptualization. **Matthew D. Jones:** Writing – review & editing, Conceptualization. **Albert Nkwasa:** Writing – review & editing. **Aristeidis Koutroulis:** Writing – review & editing. **Hannes Müller Schmied:** Writing – review & editing. **Hong-Yi Li:** Writing – review & editing. **Hyungjun Kim:** Writing – review & editing. **Naota Hanasaki:** Writing – review & editing. **Rohini Kumar:** Writing – review & editing. **Wim Thiery:** Writing – review & editing. **Yadu Pokhrel:** Writing – review & editing.

Declaration of competing interest

The authors declare that they have no known competing financial interests or personal relationships that could have appeared to influence the work reported in this paper.

Data availability

Data will be made available on request.

References

Aeschbach-Hertig, W., Gleeson, T., 2012. Regional strategies for the accelerating global problem of groundwater depletion. Nat. Geosci. 5 (12), 853–861.

Alencar, A.A., et al., 2015. Landscape fragmentation, severe drought, and the new Amazon forest fire regime. Ecol. Appl. 25 (6), 1493–1505.

Andreadis, K.M., et al., 2005. Twentieth-century drought in the conterminous United States. J. Hydrometeorol. 6 (6), 985–1001.

Barber, V.A., Juday, G.P., Finney, B.P., 2000. Reduced growth of Alaskan white spruce in the twentieth century from temperature-induced drought stress. Nature 405 (6787), 668–673.

Beguería, S., Vicente-Serrano, S.M., Beguería, M.S., 2017. Package "spei". In: Calculation of the Standardised Precipitation-Evapotranspiration Index.

Bisht, D.S., et al., 2019. Drought characterization over India under projected climate scenario. Int. J. Climatol. 39 (4), 1889–1911.

Brutsaert, W., 2005. Hydrology: An Introduction. Cambridge University Press.

Cavledes, C.N., 1985. Emergency and institutional crisis in Peru during El Niño 1982–1983. Disasters 9 (1), 70–74.

Csank, A.Z., et al., 2016. Tree-ring isotopes reveal drought sensitivity in trees killed by spruce beetle outbreaks in south-central Alaska. Ecol. Appl. 26 (7), 2001–2020.

Dahal, P., et al., 2016. Drought risk assessment in central Nepal: temporal and spatial analysis. Nat. Hazards 80 (3), 1913–1932.

Dai, A., 2011. Drought under global warming: a review. Wiley Interdiscip. Rev. Clim. Chang. 2 (1), 45–65.

Das, P.K., et al., 2016. Trends and behaviour of meteorological drought (1901–2008) over Indian region using standardized precipitation–evapotranspiration index. Int. J. Climatol. 36 (2), 909–916.

Diaz, V., et al., 2020. Characterisation of the dynamics of past droughts. Sci. Total Environ. 718, 134588.

Eng, K., Milly, P.C.D., 2007. Relating low-flow characteristics to the base flow recession time constant at partial record stream gauges. Water Resour. Res. 43 (1).

Field, R.D., et al., 2004. A drought-based predictor of recent haze events in western Indonesia. Atmos. Environ. 38 (13), 1869–1878.

Flatau, M.K., et al., 2003. Delayed onset of the 2002 Indian monsoon. Geophys. Res. Lett. 30 (14).

Ge, Y., Apurv, T., Cai, X., 2016. Spatial and temporal patterns of drought in the Continental US during the past century. Geophys. Res. Lett. 43 (12), 6294–6303.

Glazovsky, N., 2009. Combat desertification, deforestation and drought. In: Area Studies (Regional Sustainable Development Review): Russia-Volume I, p. 143.

Gleeson, T., et al., 2014. A glimpse beneath earth's surface: GLobal HYdrogeology MaPS (GLHYMPS) of permeability and porosity. Geophys. Res. Lett. 41 (11), 3891–3898.

Gocic, M., Trajkovic, S., 2014. Spatiotemporal characteristics of drought in Serbia. J. Hydrol. 510, 110–123.

Gosling, S., et al., 2017. ISIMIP2a Simulation Data From Water (Global) Sector. https://doi.org/10.5880/PIK.2017.010.

Guo, H., et al., 2018. Space-time characterization of drought events and their impacts on vegetation in Central Asia. J. Hydrol. 564, 1165–1178.

Hanasaki, N., et al., 2018. A global hydrological simulation to specify the sources of water used by humans. Hydrol. Earth Syst. Sci. 22 (1). https://doi.org/10.5194/hess-22-789-2018.

Hannaford, J., et al., 2011. Examining the large-scale spatial coherence of European drought using regional indicators of precipitation and streamflow deficit. Hydrol. Process. 25 (7), 1146–1162.

Haslinger, K., et al., 2014. Exploring the link between meteorological drought and streamflow: effects of climate-catchment interaction. Water Resour. Res. 50 (3), 2468–2487.

Hatmoko, W., et al., 2015. Monitoring and prediction of hydrological drought using a drought early warning system in Pemali-Comal river basin, Indonesia. Procedia Environ. Sci. 24, 56–64.

Herrera-Estrada, J.E., Satoh, Y., Sheffield, J., 2017. Spatiotemporal dynamics of global drought. Geophys. Res. Lett. 44 (5), 2254–2263.

Huntington, J.L., Niswonger, R.G., 2012. Role of surface-water and groundwater interactions on projected summertime streamflow in snow dominated regions: an integrated modeling approach. Water Resour. Res. 48 (11).

Joseph, S., Sahai, A.K., Goswami, B.N., 2009. Eastward propagating MJO during boreal summer and Indian monsoon droughts. Clim. Dyn. 32 (7), 1139–1153.

Keil, A., et al., 2008. What determines farmers' resilience towards ENSO-related drought? An empirical assessment in Central Sulawesi, Indonesia. Clim. Chang. 86 (3), 291–307.

Kingston, D.G., et al., 2013. Ocean–atmosphere forcing of summer streamflow drought in Great Britain. J. Hydrometeorol. 14 (1), 331–344.

Kingston, D.G., et al., 2015. European-scale drought: understanding connections between atmospheric circulation and meteorological drought indices. J. Clim. 28 (2), 505–516.

Kumar, A., et al., 2022. Multi-model evaluation of catchment-and global-scale hydrological model simulations of drought characteristics across eight large river catchments. Adv. Water Resour. 165, 104212.

Lettenmaier, D.P., Wood, E.F., Parkinson, D.B., 1990. Operating the Seattle water system during the 1987 drought. J. Am. Water Works Assoc. 82 (5), 55–60.

Li, W., et al., 2008. Observed change of the standardized precipitation index, its potential cause and implications to future climate change in the Amazon region. Philos. Trans. R. Soc. B 363 (1498), 1767–1772.

Liang, X., et al., 1994. A simple hydrologically based model of land surface water and energy fluxes for general circulation models. J. Geophys. Res. https://doi.org/10.1029/94jd00483.

Limsakul, A., et al., 2011. PDSI-based variations of droughts and wet spells in Thailand: 1951–2005. Environ. Asia 4 (1), 12–20.

Liu, Y., et al., 2019. Understanding the spatiotemporal links between meteorological and hydrological droughts from a three-dimensional perspective. J. Geophys. Res. Atmos. https://doi.org/10.1029/2018JD028947.

Lloyd-Hughes, B., 2012. A spatio-temporal structure-based approach to drought characterisation. Int. J. Climatol. 32 (3), 406–418.

Loaiza Cerón, W., et al., 2020. Spatio-temporal analysis of the droughts in Cali, Colombia and their primary relationships with the El Nino-Southern Oscillation (ENSO) between 1971 and 2011. Atmosfera 33 (1), 51–69.

Masih, I., et al., 2014. A review of droughts on the African continent: a geospatial and long-term perspective. Hydrol. Earth Syst. Sci. 18 (9), 3635–3649.

McKee, T.B., Doesken, N.J., Kleist, J., 1993. The relationship of drought frequency and duration to time scales. In: Proceedings of the 8th Conference on Applied Climatology. Boston, pp. 179–183.

Mishra, A.K., Singh, V.P., 2010. A review of drought concepts. J. Hydrol. https://doi.org/10.1016/j.jhydrol.2010.07.012 ee.

Mortensen, E., et al., 2018. Regression-based season-ahead drought prediction for southern Peru conditioned on large-scale climate variables. Hydrol. Earth Syst. Sci. 22 (1), 287–303.

Muller Schmied, H., et al., 2016. Variations of global and continental water balance components as impacted by climate forcing uncertainty and human water use. Hydrol. Earth Syst. Sci. 20 (7). https://doi.org/10.5194/hess-20-2877-2016.

Nasrati, R., 2018. Signs of climate change in Afghanistan: drought and its effect on agriculture. Региональные проблеМы 21 (3 (1)), 75–81.

Ndehedehe, C.E., et al., 2019. Modelling the impacts of global multi-scale climatic drivers on hydro-climatic extremes (1901–2014) over the Congo basin. Sci. Total Environ. 651, 1569–1587.

Nicklen, E.F., et al., 2019. Stand basal area and solar radiation amplify white spruce climate sensitivity in interior Alaska: evidence from carbon isotopes and tree rings. Glob. Chang. Biol. 25 (3), 911–926.

Parry, S., et al., 2012. Multi-year droughts in Europe: analysis of development and causes. Hydrol. Res. 43 (5), 689–706.

Peters, E., et al., 2006. Propagation and spatial distribution of drought in a groundwater catchment. J. Hydrol. 321 (1–4), 257–275.

Rahman, M.R., Lateh, H., 2016. Meteorological drought in Bangladesh: assessing, analysing and hazard mapping using SPI, GIS and monthly rainfall data. Environ. Earth Sci. 75 (12), 1–20.

Rathjens, C., 1975. Witterungsbedingte Schwankungen der Ernährungsbasis in Afghanistan (Alternations of the nutrition basis caused by weather conditions in Afghanistan). Erdkunde 182–188.

Riebsame, W.E., Changnon, S.A., Karl, T.R., 2019. Drought and Natural Resources Management in the United States: Impacts and Implications of the 1987–89 Drought. Routledge.

Rodda, J.C., Marsh, T.J., 2011. The 1975-76 drought-a contemporary and retrospective review. In: National Hydrological Monitoring Programme Series.

Saatchi, S., et al., 2013. Persistent effects of a severe drought on Amazonian forest canopy. Proc. Natl. Acad. Sci. 110 (2), 565–570.

Saji, N.H., et al., 1999. A dipole mode in the tropical Indian Ocean. Nature 401 (6751), 360–363.

Schewe, J., Levermann, A., 2012. A statistically predictive model for future monsoon failure in India. Environ. Res. Lett. 7 (4), 44023.

Sheffield, J., Wood, E.F., 2012. Drought: Past Problems and Future Scenarios. Routledge.

Sheffield, J., et al., 2009. Global and continental drought in the second half of the twentieth century: severity–area–duration analysis and temporal variability of large-scale events. J. Clim. 22 (8), 1962–1981.

Shukla, S., Steinemann, A.C., Lettenmaier, D.P., 2011. Drought monitoring for Washington State: indicators and applications. J. Hydrometeorol. 12 (1), 66–83.

Sigdel, M., Ikeda, M., 2010. Spatial and temporal analysis of drought in Nepal using standardized precipitation index and its relationship with climate indices. J. Hydrol. Meteorol. 7 (1), 59–74.

Sitch, S., et al., 2003. Evaluation of ecosystem dynamics, plant geography and terrestrial carbon cycling in the LPJ dynamic global vegetation model. Glob. Chang. Biol. 9 (2). https://doi.org/10.1046/j.1365-2486.2003.00569.x.

Slik, J.W.F., 2004. El Nino droughts and their effects on tree species composition and diversity in tropical rain forests. Oecologia 141 (1), 114–120.

Sori, R., et al., 2021. Spatiotemporal Variability of Droughts in the Congo River Basin: The Role of Atmospheric Moisture Transport.

Spinoni, J., et al., 2015. The biggest drought events in Europe from 1950 to 2012. J. Hydrol. Reg. Stud. 3, 509–524.

Stoelzle, M., et al., 2014. Streamflow sensitivity to drought scenarios in catchments with different geology. Geophys. Res. Lett. 41 (17), 6174–6183.

Takata, K., Emori, S., Watanabe, T., 2003. Development of the minimal advanced treatments of surface interaction and runoff. Glob. Planet. Chang. 38 (1–2). https://doi.org/10.1016/S0921-8181(03)00030-4.

Tallaksen, L.M., Stahl, K., 2014. Spatial and temporal patterns of large-scale droughts in Europe: model dispersion and performance. Geophys. Res. Lett. 41 (2), 429–434.

Tang, Q., et al., 2007. The influence of precipitation variability and partial irrigation within grid cells on a hydrological simulation. J. Hydrometeorol. https://doi.org/10.1175/JHM589.1.

Tanguy, M., et al., 2021. Regional differences in spatiotemporal drought characteristics in Great Britain. Front. Environ. Sci. 9.
Teuling, A.J., et al., 2013. Evapotranspiration amplifies European summer drought. Geophys. Res. Lett. 40 (10), 2071–2075.
Utkuzova, D.N., Han, V.M., Vil'fand, R.M., 2015. Statistical analysis of extreme drought and wet events in Russia. Atmos. Ocean. Opt. 28 (4), 336–346.
van Lanen, H.A.J., et al., 2004. Flow generating processes. In: Hydrological Drought. Processes and Estimation Methods for Streamflow and Groundwater, pp. 53–96.
van Loon, A.F., 2013. On the Propagation of Drought: How Climate and Catchment Characteristics Influence Hydrological Drought Development and Recovery.
Van Loon, A.F., 2015. Hydrological drought explained. In: Wiley Interdisciplinary Reviews: Water. https://doi.org/10.1002/wat2.1085.
Van Loon, A.F., Van Lanen, H.A.J., 2012. A process-based typology of hydrological drought. Hydrol. Earth Syst. Sci. 16 (7), 1915–1946.
Van Nieuwstadt, M.G.L., Sheil, D., 2005. Drought, fire and tree survival in a Borneo rain forest, East Kalimantan, Indonesia. J. Ecol. 93 (1), 191–201.
Verbyla, D., 2008. The greening and browning of Alaska based on 1982–2003 satellite data. Glob. Ecol. Biogeogr. 17 (4), 547–555.
Verdon-Kidd, D.C., Kiem, A.S., 2014. Synchronicity of historical dry spells in the Southern Hemisphere. Hydrol. Earth Syst. Sci. 18 (6), 2257–2264.
Vicente-Serrano, S.M., 2006. Differences in spatial patterns of drought on different time scales: an analysis of the Iberian Peninsula. Water Resour. Manag. 20 (1), 37–60.
Vicente-Serrano, S.M., López-Moreno, J.I., 2005. Hydrological response to different time scales of climatological drought: an evaluation of the Standardized Precipitation Index in a mountainous Mediterranean basin. Hydrol. Earth Syst. Sci. 9 (5), 523–533.
Vicente-Serrano, S.M., et al., 2015. Spatio-temporal variability of droughts in Bolivia: 1955–2012. Int. J. Climatol. 35 (10), 3024–3040.
Vidal, J.P., et al., 2010. Multilevel and multiscale drought reanalysis over France with the Safran-Isba-Modcou hydrometeorological suite. Hydrol. Earth Syst. Sci. 14 (3), 459–478.
Wada, Y., Wisser, D., Bierkens, M.F.P., 2014. Global modeling of withdrawal, allocation and consumptive use of surface water and groundwater resources. Earth Syst. Dyn. https://doi.org/10.5194/esd-5-15-2014.
Wang, K., et al., 2015. Analysis of spatio-temporal evolution of droughts in Luanhe River Basin using different drought indices. Water Sci. Eng. 8 (4), 282–290.
Wattanakij, N., Thavorntam, W., Mongkolsawat, C., 2006. Analyzing spatial pattern of drought in the northeast of Thailand using multi-temporal standardized precipitation index (SPI). In: Proceedings of the 27th Asean Conference on Remote Sensing.
Weedon, G.P., et al., 2011. Creation of the WATCH forcing data and its use to assess global and regional reference crop evaporation over land during the twentieth century. J. Hydrometeorol. 12 (5). https://doi.org/10.1175/2011JHM1369.1.
Wilhite, D.A., Glantz, M.H., 1985. Understanding: the drought phenomenon: the role of definitions. Water Int. 10 (3), 111–120.
Wong, G., Van Lanen, H.A.J., Torfs, P., 2013. Probabilistic analysis of hydrological drought characteristics using meteorological drought. Hydrol. Sci. J. 58 (2), 253–270.
Wu, J., et al., 2018. Meteorological and hydrological drought on the Loess Plateau, China: evolutionary characteristics, impact, and propagation. J. Geophys. Res. Atmos. 123 (20), 11–569.
Xiao, J., Zhuang, Q., 2007. Drought effects on large fire activity in Canadian and Alaskan forests. Environ. Res. Lett. 2 (4), 44003.
Xiao, M., et al., 2016. Transitional properties of droughts and related impacts of climate indices in the Pearl River basin, China. J. Hydrol. 534, 397–406.
Xu, K., et al., 2015. Spatio-temporal variation of drought in China during 1961–2012: a climatic perspective. J. Hydrol. 526, 253–264.
Yuan, X., et al., 2017. Understanding and seasonal forecasting of hydrological drought in the Anthropocene. Hydrol. Earth Syst. Sci. 21 (11), 5477–5492.
Zhan, W., et al., 2016. Depiction of drought over sub-Saharan Africa using reanalyses precipitation data sets. J. Geophys. Res. Atmos. 121 (18), 10–555.
Zhu, Y., et al., 2016. Combined use of meteorological drought indices at multi-time scales for improving hydrological drought detection. Sci. Total Environ. 571, 1058–1068.